

## Removal of Hexavalent Chromium using a PVDF-based Polymer Inclusion Membrane with a phosphonium-based ionic liquid

Mochamad L. Firmansyah<sup>1,\*</sup>, Zahra Salsabilla<sup>1</sup>, Nuzula T.S. Andika<sup>1</sup>, Vania G. Prasetyo<sup>1</sup>, Yonathan S. Ardian<sup>1</sup>, Muhammad H. Yahya<sup>1</sup>

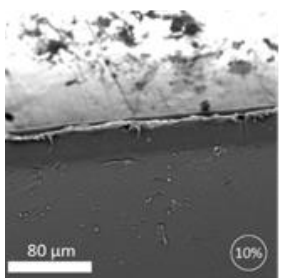
<sup>1</sup> Nanotechnology Engineering, Faculty of Advanced Technology and Multidisciplinary, Airlangga University, Jl. Dr. Ir. H. Soekarno, Surabaya 60115, Indonesia

\*Corresponding Author: [ml.firmansyah@fmm.unair.ac.id](mailto:ml.firmansyah@fmm.unair.ac.id)

### Article history:

Received 19 January 2023

Accepted 1 March 2023



### ABSTRACT

Hexavalent chromium (Cr(VI)) is widely used in industrial processes and products while it possess a severe health effect on living being and environmental hazard. Removing Cr(VI) from industrial wastewater and other contaminated sources is important for human health and the ecosystem. Various treatment technologies have been developed to remove it, but further research is needed to improve their effectiveness. This report discusses the adsorption of Cr(VI) using a phosphonium-based ionic liquid, trioctyldecylphosphonium chloride, in a polymer inclusion membrane (PIM) matrix. The PIM's chemical structure was also examined by FTIR spectroscopy, and a cross-sectional SEM image was taken. The adsorption efficiency of PIM increases as the IL content increase and experiencing a significant jump 3in over 30% of IL content. The maximum adsorption capacity corresponds to PIM40 and PIM50, which showed a 90% adsorption in 24 hours. However, PIM50 was difficult to regenerate and reuse due to membrane stability. Cr(VI) adsorption by PIM40 followed a pseudo-second-order kinetic model and Langmuir isotherm model with adsorption capacity of 74.1 mg g<sup>-1</sup>. Following the isotherm model, the adsorption of Cr(VI) probably through an anionic exchange between IL in the PIM and Cr(VI) complex. Cr(VI) desorption from PIM40 was carried out by using a 0.5 mol L<sup>-1</sup> NaNO<sub>3</sub>. The PIM40 was able to be reused for five times without a significant change in the performance. This study has shown that PIM can effectively remove heavy metals from water and selectively remove specific contaminants. PIM are also relatively easy to regenerate or replace, making them a potentially cost-effective method for removing heavy metals from water.

**Keywords:** Water pollution, Ionic Liquid, Adsorption, Polymer Inclusion Membrane, Chromium

© 2023 School of Chemical and Engineering, UTM. All rights reserved  
| eISSN 0128-2581 |

## 1. INTRODUCTION

Hexavalent chromium (Cr(VI)) is a highly toxic and carcinogenic form of chromium that is widely used in industrial processes and products. Exposure to Cr(VI) can occur through inhalation, ingestion, and dermal contact. It has been linked to various negative health effects, including respiratory and cardiovascular problems, DNA damage, and increased cancer risk [1]. Indonesia's regulations stipulate that the permissible limit of Cr(VI) in industrial and domestic wastewater are 0.4 and 1 mg L<sup>-1</sup>, respectively [2]. Cr(VI) presence in the environment and various products has raised concerns about the potential impact on human health. In addition to its toxic effects, Cr(VI) can negatively impact the ecosystem, as it can bioaccumulate in the food chain and cause harm to aquatic life [1].

Therefore, removing Cr(VI) from industrial wastewater and other contaminated sources is of great importance. Several treatment technologies, including adsorption, chemical reduction, and electrochemical reduction, have been developed to remove Cr(VI) from aqueous solutions [3]. However, the effectiveness of these methods can vary, and there is a need for further research to improve Cr(VI) removal from contaminated sources. Cr(VI) can be adsorbed onto various adsorbents, including activated carbon, zeolites, and metal oxides [4]. In addition, liquid membrane techniques such as supported liquid membranes have also been explored to remove Cr(VI) [3]. These techniques have advantages over conventional solvent extraction but also have limitations restricting their industrial use.

Recently, polymer inclusion membranes (PIMs) have been explored for metal removal techniques, offering the

benefits of other liquid membrane technologies. The key components of PIMs are base polymer, extractant, and plasticizer. In recent years, poly(vinylidene fluoride-co-hexafluoropropylene) (PVDF-HFP) has been explored extensively as PIMs base polymer along with poly(vinyl chloride) (PVC) and cellulose triacetate (CTA) [5]. PVDF-HFP has several advantages compared to other polymer, such as high hydrophobicity, good stability, high chemical resistance, and highly soluble in tetrahydrofuran, often used to prepare membrane casting solutions [6]. PIMs consist of a polymer matrix containing a specific type of ligand or functional group capable of selectively binding to and removing the target contaminant from the solution. Studies have shown that PIMs can effectively remove heavy metals from water, with high removal efficiencies and low leaching of the metals from the membrane [7]. PIMs have the advantage of being able to selectively remove specific contaminants from water while allowing other components of the water to pass through the membrane. They are also relatively easy to regenerate or replace, making them a potentially cost-effective method for removing heavy metals from water. In addition to their use for removing heavy metals from water, PIMs have also been studied to remove other types of contaminants, including dyes, pesticides, and pharmaceuticals, from water and other liquids [8]. Moreover, various chemical additives have been used to alter the PIM adsorption capacity for various adsorbates. One of these modifications is grafting ionic liquid to improve the adsorbent capability. Ionic liquid (IL) has been tested using solvent or membrane extraction methods in precious metal extraction. However, IL has a significant drawback due to its high viscosity, which leads to the use of a large amount of volatile organic compounds (VOCs).

Thus, PIM containing a phosphonium-based IL, trioctyldecylphosphonium chloride was used to remove Cr(IV) from the aqueous solution. This report also explores the effect of PIM composition on removal efficiency. A desorption and regeneration study were also conducted to evaluate the longevity of the PIM.

## 2. MATERIALS AND METHODS

### 2.1 Materials

2-nitrophenyloctylether (2NPOE, 99%), sodium hydroxide (NaOH), HNO<sub>3</sub> (65%), CS(NH<sub>2</sub>)<sub>2</sub> (98%), H<sub>2</sub>SO<sub>4</sub> (98%), Na<sub>2</sub>SO<sub>3</sub> (99%), and tetrahydrofuran (THF, 99.5%) were purchased from Merck & Co., Inc. NaNO<sub>3</sub>, poly(vinylidene fluoride-co-hexafluoropropylene) (PVDF-HFP), and K<sub>2</sub>Cr<sub>2</sub>O<sub>7</sub> (99%) were purchased from Sigma-Aldrich. Other solution was prepared by using a double distilled water.

### 2.2 Preparation of polymer inclusion membrane

To create the PIMs, a mixture of P<sub>8,8,8,12</sub>Cl and PVDF-HFP was dissolved and stirred in THF (15 mL) until

homogeneous. The homogeneous mixture was poured onto a petri dish with a 8 cm diameter ring. The petri dish was then covered and stacked with weight to allow the slow evaporation of THF. Once the PIMs were completely dried, they were carefully removed from the cast. The PIMs was denoted following their IL content (10% IL = PIM10, 20% IL = PIM20, 30% IL = PIM30, 40% IL = PIM40, 50% IL = PIM50).

### 2.3 Batch adsorption and desorption of Cr(VI)

A 100 mg segment of the PIM was placed in a container with 50 mL of Cr(VI) solution (100 mg L<sup>-1</sup>). The container was shaken at 90 rpm using a linear shaker (DLAB SK-L180-E) for 24 hours. The PIM containing Cr(VI) was then removed from the solution and air-dried. A desorption experiment was performed by mixing a Cr(VI)-containing PIM was mixed with 50 mL of desorption solution and shaking it in the same manner as the extraction process for another 24 hours. The adsorption (E) and desorption (D) efficiencies were calculated using Eq. (1) and (2), respectively.

$$E (\%) = \frac{(C_{F,i} - C_{F,f})}{C_{F,i}} \times 100 \quad (1)$$

$$D (\%) = \frac{C_{S,f}}{(C_{F,i} - C_{F,f})} \times 100 \quad (2)$$

Where, C<sub>F,i</sub>, C<sub>F,f</sub>, and C<sub>S,f</sub> represent the Cr(VI) concentration in the solution before and after adsorption process, and Cr(VI) concentration in the stripping solution, respectively.

### 2.4 Cr(VI) Concentration Determination

Diphenylcarbazide (DPC) was used to complex with Cr(VI), and the resulting complex showed a purple color. The Cr(VI)-containing solution was mixed with the appropriate indicator, and the absorbance was measured at 540 nm. All spectra measurements were done in triplicate to ensure the spectra stability and minimize errors.

### 2.5 Characterization

The chemical structure of the PIM was analyzed using a Fourier transform infrared (FTIR) spectrometer (Thermo Scientific, Nicolet iS 10). A scanning electron microscope with an energy-dispersive X-ray (SEM-EDX, Thermo Scientific, Phenom Desktop ProXL) was used to analyze the PIM morphology and elemental mapping. A Thermo Scientific GENESYS UV-Vis Spectrophotometer was used to perform the spectrophotometric analysis. The absorbance of the solutions was measured using a 1-cm-thick quartz cell and double-distilled water as a blank.

## 3. RESULTS AND DISCUSSION

### 3.1 Physicochemical properties of PIM

The  $P_{8,8,8,12}Cl$  compound was analyzed using  $^{13}C$  and  $^{31}P$  NMR spectroscopy as shown in Figure 1A and B. The  $^{31}P$  NMR spectra in Figure 1A showed a single peak at 34.20 ppm, indicating no oxidation was present in the synthesis process [9]. The chemical composition of  $P_{8,8,8,12}Cl$  was found to be consistent with the calculated values (C, 12.10; H, 65.14, N, 0.00) and the experimental results (C, 12.05; H, 66.91; N, 0.02).

The chemical structure of the membrane was analyzed using FTIR spectroscopy. Figure 1C and D show the spectra of PIMs with different IL compositions. The spectra of the PIMs showed peaks at  $722\text{ cm}^{-1}$ ,  $1075\text{ cm}^{-1}$ , around  $2900\text{ cm}^{-1}$ , and  $1435\text{ cm}^{-1}$ , which is attributed to the P-C, C-C, C-H stretching; and P-CH<sub>2</sub>-R bending vibration originating from the  $P_{8,8,8,12}Cl$  structure [10]. The absorbance peak related to PVDF-HFP were particularly notable in the  $4500\text{--}1500\text{ cm}^{-1}$  region (indicated in red) and were dominant in the infrared spectra of the PIM [11]. As

the IL composition increased, the signature peak of PVDF-HFP, which was indicated in red showed a slight decreased as the IL content increase. In addition, significant increase was observed in around  $2900\text{ cm}^{-1}$  (Figure 1D), originating from  $P_{8,8,8,12}Cl$  long aliphatic chain, due to the increase in  $P_{8,8,8,12}Cl$  presence in the membrane. Due to issues with membrane physical stability, FTIR spectra of PIM50 was not collected and presented.

Figure 2 presents a SEM image of the membrane cross-section. The image shows that the PIM has a dense morphology across different IL compositions. However, the membrane texture becomes slightly coarser as the IL composition increases. This could be caused by the inhibition of polymerization due to a high concentration of IL in the membrane [12].

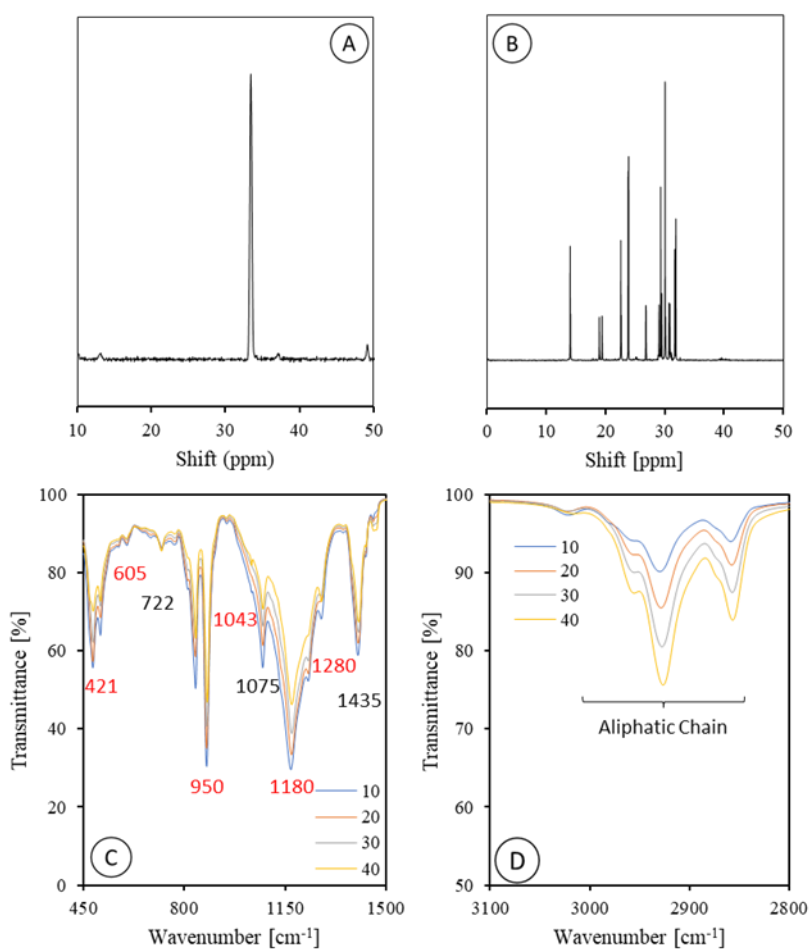


**Figure 1** (A)  $^{31}P$  NMR and (B)  $^{13}C$  NMR of  $P_{8,8,8,12}Cl$ ; (C) and (D) FTIR spectra of PIM with different  $P_{8,8,8,12}Cl$  composition.

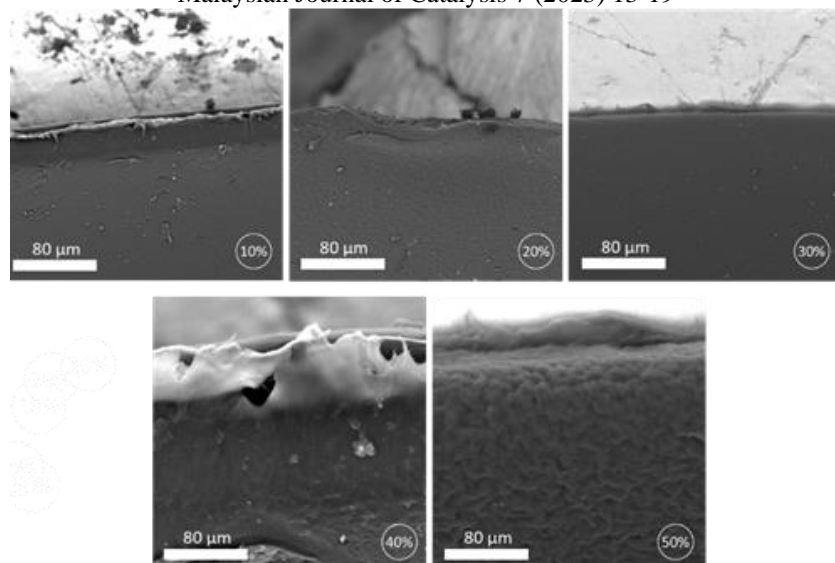


**Figure 2** SEM images of PIM with different P8,8,8,12Cl composition.

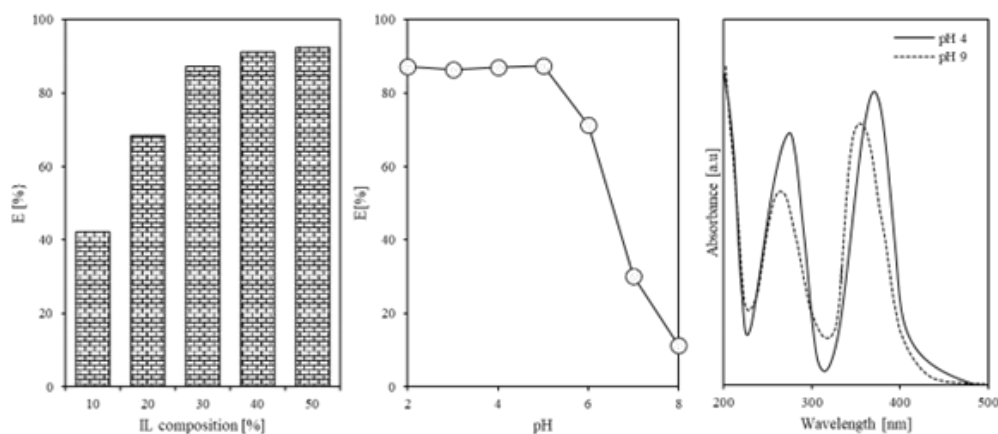


**Figure 3** Cr(VI) adsorption with the effect of (A) IL composition in PIM, and (B) pH; (C) UV-vis spectrum of Cr(VI) solution in different pH.

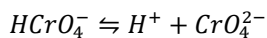
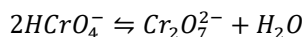
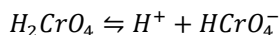
### 3.2 Adsorption Behavior of Cr(VI)

Initially, Cr(VI) adsorption on PIMs with different IL concentrations were conducted. Cr(VI) retention in the PIMs shows a positive trend with the increase of IL content. The highest adsorption efficiency was shown by PIM with almost 90% adsorption in 24 hours. However, PIM50 was difficult to use and extract from the feed solution. Significant increase in the Cr(VI) adsorption with IL increase was due to the IL concentration threshold required to create a continuous pathway into the inside matrix of the PIM, which allows the transfer of Cr(VI) ions from the surface of the PIM to the IL inside the PIM matrix [13]. Thus, due to the limited amount of IL in PIM10 and PIM20, Cr(VI) adsorption was only limited to the surface of PIM. In PIM40, the continuous pathway are fully formed in the PIM matrix

leading to the significant increase in Cr(VI) adsorption due to the ability to transfer Cr(VI) into the inside PIM matrix. A further increase in the IL content of PIM only increases the adsorption efficiency slightly. This could be due to the voluminous aliphatic groups of P<sub>8,8,8,12</sub>Cl creating steric hindrance for Cr(VI) to access the adsorption sites of PIM [14]. Therefore, PIM40 is deemed the optimal composition for Cr(VI) adsorption, and used in the subsequent adsorption experiments.

The solution pH could affect the adsorption efficiency by altering the surface charge of the adsorbent. Therefore, 100 mg of PIM40 was mixed with a Cr(VI)-containing solution (100 mg L<sup>-1</sup>) with pH variation between 2.0 to 8.0. Cr(VI) adsorption shows a constant level until pH of 5.0 and shows a significant decrease in the pH above 5.0. The equilibrium between different complexes of Cr(VI),

such as  $\text{HCrO}_4^-$ ,  $\text{Cr}_2\text{O}_7^{2-}$ , and  $\text{CrO}_4^{2-}$ , can be represented as follows.



The composition Cr(VI) complexes in the aqueous solution was analyzed by using UV-vis spectrophotometer, as depicted in Figure 3C. The solution containing Cr(VI) in acidic conditions exhibits two peaks at around 250 and 350 nm. However, in the high pH condition the absorbance peak shows a red shift indicating the presence of different Cr(VI) complexes in neutral and basic conditions [15]. The  $\text{CrO}_4^{2-}$  complex is primarily found in basic and neutral conditions, while the  $\text{HCrO}_4^-$  and  $\text{Cr}_2\text{O}_7^{2-}$  complexes are primarily found in acidic conditions. Cr(VI) adsorption onto PIM40 occurs following electrostatic interaction between the anionic moieties of IL and Cr(VI) complex. A decrease in the pH above 5.0 was likely due to a change in the surface charge. Thus, the results indicate that the optimal pH for Cr(VI) adsorption on PIM40 is 5.0 and it will be used in the proceeding experiment.

### 3.3 Kinetic and Isotherm adsorption of Cr(VI)

The batch extraction process was used to conduct both kinetic and isothermal studies. Cr(VI) adsorption kinetics by PIM40 was studied over 24 hours. The pseudo-second-order kinetic model was used to evaluate the kinetics of Cr(VI) adsorption [16]. The Cr(VI) adsorption behavior was also determined using Langmuir, Freundlich, and Temkin models [17], [18]. The equations for the kinetic and isotherm models are presented in Eq. (6) and (7-9), respectively.

$$\frac{t}{q_t} = \frac{1}{K_2 q_{eq}^2} + \frac{1}{q_{eq}} t \tag{6}$$

$$\frac{1}{q_{eq}} = \frac{1}{q_o} + \frac{1}{q_o K_L C_{eq}} \tag{7}$$

$$\log q_{eq} = \log K_F + \left(\frac{1}{n}\right) \log C_{eq} \tag{8}$$

$$q_{eq} = \frac{RT}{b_T} \ln A_T + \frac{RT}{b_T} \ln C_{eq} \tag{9}$$

Cr(VI) adsorbed at specific periods dan equilibrium were denoted as  $q_t$  and  $q_{eq}$ , respectively.  $K_2$  was the pseudo-second-order kinetic constants.  $K_L$  ( $\text{L mg}^{-1}$ ),  $K_F$ , and  $b_T$  ( $\text{kJ mol}^{-1}$ ) were attributed to the Langmuir, Freundlich, and Temkin constants, respectively. The other model parameters were explained as,  $q_o$  ( $\text{mg g}^{-1}$ ): adsorption capacity,  $n$ : the adsorption favorability,  $A_T$  ( $\text{L g}^{-1}$ ): equilibrium binding constant. In the kinetic experiment, PIM40 reached equilibrium adsorption in 350 minutes, which was used in subsequent experiments. The Cr(VI) adsorption kinetics was well-fitted with the pseudo-second-order kinetic model, with

a high  $R_2$  value and comparable  $q_{eq}$  values (Table 1). This suggests that Cr(VI) adsorption was rate-limited by the chemical interactions between the adsorbent and adsorbate. (3)

Table 1 shows the parameters obtained from the concentration variation experiment. Cr(VI) adsorption onto PIM40 appears to follow a monolayer adsorption pathway, as the Langmuir model had a higher  $R^2$  value than the Freundlich model. The  $n$ -factor from the Freundlich model suggests a favorable interaction between Cr(VI) and PIM40. The Temkin model can determine if the adsorption pathway is physisorption or chemisorption. The Cr(VI) adsorption appears to be a chemisorption process, as the  $b_T$  from the Temkin model is  $65.5 \text{ kJ mol}^{-1}$  [19]. Based on the kinetic results, it is likely that the chemical adsorption of Cr(VI) onto PIM40 occurs through ion exchange between the anionic complex and the anion of the IL. The Langmuir model had a better fit between experimental and calculated  $q_{eq}$  values.

**Table 1** Properties of the catalysts

PIM40	Parameters	Value
Langmuir	$q_o$	74.1
	$K_L$	0.026
	$R^2$	0.998
Freundlich	$K_F$	6.21
	$n$	2.38
	$R^2$	0.929
Temkin	$A_T$	2.05
	$b_T$	65.5
	$R^2$	0.987
Pseudo-second order kinetic	$K_2$	0.039
	$q_{eq,exp}$	10.9
	$q_{eq,cal}$	10.5
	$R^2$	0.998

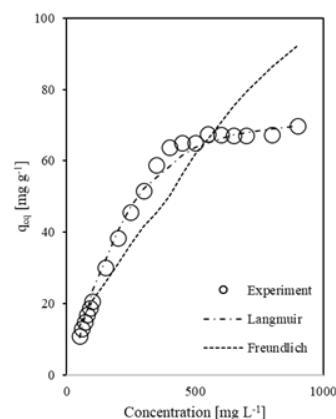


**Figure 4** Comparison of experimental data with Langmuir and Freundlich model for PIM40

Figure 4 compares the Langmuir, Freundlich isotherm models data and the experimental data. The experimental

data suitably fit with the Langmuir isotherm models, as indicated by the high  $R^2$  value. This means that the way Cr(VI) adsorbed onto PIM40 is through a single layer of chemical bonding, and that there is a favorable interaction between the two components.

### 3.4 Desorption and Regeneration

The PIM40 used in the desorption process contained 19 mg Cr(VI) per 1 g of PIM. The desorption efficiency of various solution was presented in Table 2. The highest desorption efficiency was presented by NaOH solutions, followed by  $\text{NaNO}_3$ . However, physical changes in PIM40 were observed after desorption using NaOH. The membrane turned dark brown after desorption which irreversibly affect the PIM40 performance in the subsequent adsorption-desorption cycle. On the other hand, Cr(VI) desorption using  $\text{NaNO}_3$  showed less effectivity than NaOH, but significantly mild physical change. The color of the PIM40 turns to yellow during in an adsorption-desorption cycle. Furthermore, the adsorbent can be regenerated and used for subsequent cycle.

**Table 2** Cr(VI) desorption efficiency of various solutions

Desorption Solution	D(%)
0.5 mol L <sup>-1</sup> $\text{NaNO}_3$	79.2
0.5 mol L <sup>-1</sup> NaOH	90.8
0.5 mol L <sup>-1</sup> $\text{CS}(\text{NH}_2)_2$	28.1
1 mol L <sup>-1</sup> $\text{HNO}_3$	30.5
0.5 mol L <sup>-1</sup> $\text{Na}_2\text{S}_2\text{O}_3$	42.4
1 mol L <sup>-1</sup> $\text{H}_2\text{SO}_4$	7.9
1 mol L <sup>-1</sup> HCl	2.5
0.5 mol L <sup>-1</sup> $\text{Na}_2\text{SO}_3$	8.1
$\text{H}_2\text{O}$	0

The adsorption and desorption of Cr(VI) using PIM40 were carried out using a 100 mg L<sup>-1</sup> Cr(VI) feed solution and 0.5 mol L<sup>-1</sup>  $\text{NaNO}_3$  as the desorption solution. The results in Figure 5 show that PIM40 can be recycled for five cycles without experiencing a significant decline in performance. This indicates that the adsorbent is capable of performing long-term adsorption processes.

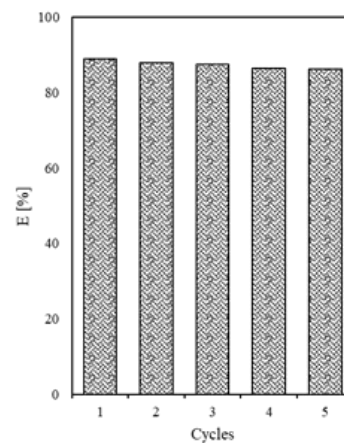


**Figure 5** Adsorption-desorption cycle of Cr(VI).

## 4. CONCLUSION

In conclusion, the use of a polymer inclusion membrane (PIM) containing a phosphonium-based ionic liquid, trioctyldecylphosphonium chloride, for the removal of Cr(VI) from an aqueous solution has been studied. Various techniques characterized the PIM, showing it was a stable and well-synthesized membrane. The results of the adsorption experiments showed that the Cr(VI) adsorption efficiency increases when the extracting agent percentage in PIM increases. The maximum adsorption capacity was reached for a PIM composition of 40-50% IL. The adsorption of Cr(VI) onto the PIM40 probably go through electrostatic static interaction with chitosan and anionic exchange with the  $\text{P}_{8,8,8,12}\text{Cl}$ . The adsorption process followed a monolayer chemisorption process was a good fit for the adsorption of Cr(VI) by both adsorbent. The pseudo-second-order kinetic model was also fairly well suited to this mechanism. PIM40 are also relatively easy to regenerate, making them a potentially cost-effective method for removing heavy metals from water. This study provides a potential solution for the removal of Cr(VI) from an aqueous solution using PIMs.

## ACKNOWLEDGEMENTS

The authors are grateful to the 2020's students of the nanotechnology study program of Universitas Airlangga for their excellent work in preparing the adsorption in the practical laboratory class.

## REFERENCES

- [1] A. S. Ayangbenro and O. O. Babalola, *Int. J. Environ. Res. Public Health*. 14 (2017).
- [2] Ministry of Environment and Forestry of The Republic of Indonesia, *Peraturan Menteri Lingkungan Hidup RI No. 5 Tahun 2014 Tentang Baku Mutu Air Limbah*. (2014) 1–83.
- [3] H. Peng and J. Guo, *Environ. Chem. Lett.* 18 (2020) 2055–2068, Nov. 2020, doi: 10.1007/s10311-020-01058-x.

- [4] Md. A. Islam, M. J. Angove, and D. W. Morton, *Environ. Nanotechnol. Monit. Manag.* 12 (2019) 100267
- [5] C. A. Carner, C. F. Croft, S. D. Kolev, and M. I. G. S. Almeida, *Sep. Purif. Technol.* 239 (2020) 116486.
- [6] S. Bahrami, M. R. Yaftian, P. Najvak, L. Dolatyari, H. Shayani-Jam, and S. D. Kolev, *Sep. Purif. Technol.* 250 (2020) 117251.
- [7] B. Keskin, B. Zeytuncu-Gökoğlu, and I. Koyuncu, *Chemosphere.* 279 (2021) 130604.
- [8] U. Kamran, K. Y. Rhee, S.-Y. Lee, and S.-J. Park, *Chemosphere.* 306 (2022) 135590.
- [9] M. L. Firmansyah, A. T. N. Fajar, R. R. Mukti, T. Ilmi, G. T. M. Kadja, and M. Goto, *Solvent Extr. Res. Dev. Jpn.* 28 (2021) 79–93.
- [10] A. T. N. Fajar, T. Hanada, and M. Goto, *J. Membr. Sci.* 629 (2021) 119296.
- [11] D. Wang, J. Liu, J. Chen, Q. Liu, and H. Zeng, *Chem. Eng. Sci.* 220 (2020) 115620.
- [12] D. Zheng *et al.*, *J. Membr. Sci.*, 636 (2021) 119551.
- [13] F. Sellami, O. Kebiche-Senhadjji, S. Marais, L. Colasse, and K. Fatyeyeva, *Sep. Purif. Technol.* 248 (2020) 117038.
- [14] M. Qiu *et al.*, *J. Membr. Sci.* 573 (2019) 1–10.
- [15] M. C. Fournier-Salaün and P. Salaün, *Cent. Eur. J. Chem.* 5 (2007) 1084–1093.
- [16] Y. S. Ho and G. McKay, *Process Biochem.* 34 (1999) 451–465.
- [17] A. O. Dada, A. P. Olalekan, A. M. Olatunya, and O. Dada, *IOSR J. Appl. Chem.* 3 (2012) 38–45.
- [18] A. A. Inyinbor, F. A. Adekola, and G. A. Olatunji, *Water Resour. Ind.* 15 (2016) 14–27.
- [19] Y. S. Ho, J. F. Porter, and G. McKay, *Water. Air. Soil Pollut.* 141 (2002) 1–4.